

Article

Research on Main Engine Power of Transport Ship with Different Bows in Ice Area According to EEDI Regulation

Yu Lu, Zhuhao Gu *, Shewen Liu *, Chunxiao Wu, Wu Shao and Chuang Li

Naval Architecture and Ocean Engineering College, Dalian Maritime University, Dalian 116026, China; luyu@dmlu.edu.cn (Y.L.); wuchunxiao@dmlu.edu.cn (C.W.); 1120201818@dmlu.edu.cn (W.S.); 1120200576@dmlu.edu.cn (C.L.)

* Correspondence: 1120191611@dmlu.edu.cn (Z.G.); liushewen@dmlu.edu.cn (S.L.)

Abstract: The Energy Efficiency Design Index (EEDI) has been applied to ship carbon emission standards since 2013, ice ships subject to the Finnish Swedish Ice Class Rules (FSICR) also need to meet the requirements of EEDI. In this study, the engine power requirements by EEDI at different stages for the considered ice class ships with different ice classes (1C, 1B, 1A, 1A Super) are compared with engine power requirements obtained from the resistance calculated by FSICR or Lindqvist method. Three different bow shapes for the considered ice class ships and different pack ice coverage are studied. The results from FSICR or Lindqvist formula show that 1A Super ice classes for all considered bow shapes cannot meet the requirement by EEDI at Phase 2 and 3; For 1B and 1A class, some bow shapes can meet the EEDI requirement for all stages, but some cannot; For 1C class, all bow shapes can meet the EEDI requirements for all stages. The ship main engine power requirements under different pack ice concentration are studied and compared to EEDI requirements.

Keywords: EEDI; ice-classed vessels; ship main engine power; pack ice concentration



Citation: Lu, Y.; Gu, Z.; Liu, S.; Wu, C.; Shao, W.; Li, C. Research on Main Engine Power of Transport Ship with Different Bows in Ice Area According to EEDI Regulation. *J. Mar. Sci. Eng.* **2021**, *9*, 1241. <https://doi.org/10.3390/jmse9111241>

Academic Editors: Mikko Suominen and Fang Li

Received: 11 September 2021
Accepted: 14 October 2021
Published: 9 November 2021

Publisher's Note: MDPI stays neutral with regard to jurisdictional claims in published maps and institutional affiliations.



Copyright: © 2021 by the authors. Licensee MDPI, Basel, Switzerland. This article is an open access article distributed under the terms and conditions of the Creative Commons Attribution (CC BY) license (<https://creativecommons.org/licenses/by/4.0/>).

1. Introduction

With global warming, the Arctic sea ice coverage is gradually decreasing, and the open water area is increasing. Based on the existing observation data, some experts predict that the summer sea ice of the Arctic Ocean will disappear completely in 2040 [1]. The decrease in the area of Arctic sea ice has improved the navigability of the Arctic waterway. Thus, ice classed vessels are in demand for Arctic and also in other ice-covered waters such as Baltic Sea. But on the other hand, the navigability of the Arctic waterway and other ice-covered water will also have an impact on the ecological environment of these regions and the global climate.

According to the “IMO Second Greenhouse Gas Study”, the total CO₂ emissions of the world’s shipping industry in 2007 were 1.054 billion tons, accounting for about 3.3% of the total global CO₂ emissions. Among them, the emissions of international shipping vessels were 870 million tons, accounting for 2.7% of the total global emissions, which was 0.9% higher than the estimated data in 2000, indicating the rapid growth of emissions brought by international shipping in the past 10 years [2]. Different methods are used to reduce ship’s greenhouse gas emission. Farkas [3] studied ships operating at sea and found that antifouling coating can reduce greenhouse gas emissions. Balcombe [4] and Xing Hui [5] studied the reduction of CO₂ emissions from ships in terms of policy and technology. If effective control measures are adopted to improve the energy utilization rate of ships, emissions can be reduced by 25% to 75% [6].

IMO’s overall strategy for CO₂ emission reduction includes technical measures, operational measures and market-based measures. At present, mandatory requirements have been formulated for technical measures (Energy Efficiency Design Index (EEDI) requirements). It uses the ratio of CO₂ emissions carrying capacity as an indicator to measure the energy efficiency of ships.

The EEDI [7] has been applied to ship emission regulation since 2013. EEDI is to limit the maximum engine power for the considered ship. The EEDI requirements will tighten in three phases: Phase 1 from January 2015, Phase 2 from January 2020 and Phase 3 from January 2025 and onward. In ice covered water such as Arctic and Baltic Sea, ice classed ships are needed for safe navigation. Ice classed ships need more engine power to travel in ice. EEDI requirements will have impact on the ice classed ships engine power since EEDI requirements will reduce the maximum allowed power. Ice-class ships subject to the Finnish-Swedish Ice Class Rules (FSICR) [8] need to meet the requirements of EEDI. For ice class ships, EEDI provided correction factor so that the maximum allowed engine power can be increased for ships navigating in ice.

A number of EEDI related research projects for ice classed ships, funded by the Finnish-Swedish Winter Navigation Research Board, have been carried out. These include statistical studies on the effect of ice class correction factors for various ship hull forms [9,10] and a statistical study on the effect of EEDI on the need for icebreaker assistance [11]. Some results from these projects have been implemented in new IMO guidelines for the calculation of EEDI (IMO 2018).

To calculate the power requirement for ships traveling in ice, the ice resistance is needed. Ice resistance can be obtained by ice tank model tests [12], numerical simulation [13] and empirical formulas [14]. For quick calculation, empirical formula are more suitable for EEDI analysis. There are many empirical formulas for calculating ice-going resistance [15], such as: Lindqvist [16], Riska [17] formulas, etc. Compared with other formulas, Lindqvist formula considers more details of the bow hull form and also the ship's speed, and more widely used for ice-going resistance calculation [18]. In this study, Lindqvist and FSICR formula are used for ice resistance calculation for ships traveling in brash ice since FSICR requires ships to operate in brash ice channel opened by escorting ice-breaker. EEDI allowable maximum power requirements are calculated for considered ice class ships at different EEDI stages and for different ice classes (1C, 1B, 1A, 1A Super). Three different bow forms and different pack ice concentration are considered to calculate ship main engine power requirements, which are compared to EEDI.

2. Methods

When the ship is sailing in open water, the power of the main engine mainly depends on the open water resistance value at the maximum speed. When considering the influence of ice navigation, the ship is mainly affected by the ice resistance when navigating in the ice area. The ice resistance is the largest influencing factor of the ship design main engine power. Different hull form can produce different open water and ice resistance, thus affects the ship's allowable main engine power.

2.1. Maximum Power of the Main Engine in Open Water Area

The maximum power of the ship's main engine in open water is calculate from the total resistance in open water at the maximum speed as in Equation (1). The calculation methods of ship open water resistance mainly include either towing tank measurements or Computational Fluid Dynamics method (CFD). Nowadays, the ship resistance can be predicted accurately using CFD. This paper uses the CFD method to calculate the resistance of the ship model, and uses the conversion Equation (1) to calculate the ship's main engine power.

$$MCR = \frac{R \cdot V}{1000} \quad (1)$$

where Marine Continuous Rating (*MCR*) is the effective power of the main engine (kW), *R* is the open water resistance (kN), and *V* is the ship speed (m/s).

2.2. Main Engine Power Calculation in Ice Area

The main engine power in ice area depends on the ice resistance. In FSICR, the required main engine power is derived from the ice resistance as Equation (2):

$$P = K_e \frac{(R_{CH}/1000)^{3/2}}{D_P} [\text{kW}] \tag{2}$$

where R_{CH} is ice resistance, P is engine output power, D_P is diameter of the propeller [m]. K_e is a factor related to ship’s propellers, which shall be taken as in Table 1:

Table 1. Calculation parameter value (K_e).

Propeller Hull Form or Machinery	CP or Electric or Hydraulic Propulsion Machinery	FP Propeller
One propeller	2.03	2.26
Two propellers	1.44	1.6
Three propellers	1.18	1.31

The ship used in this paper is a single-spindle ship, and the main engine is a conventional diesel engine, so K_e takes as 2.26 and the propeller diameter D_P is 7 m. FSICR provided the formula to calculate ice resistance R_{CH} , but also accept alternative method for R_{CH} , such as model tests, CFD simulation, or other effective formulas [19]. In this study, for the calculation of ice resistance R_{CH} , the Lindqvist empirical formula method (Equation (4)) and the FSICR rules formula (Equation (5)) are used. Both of these two methods contain bow characteristics to predict the ice resistance of different bow forms. Since we only consider the Baltic ice classes (1C-1A Super) and FSICR requires icebreaker escorting, the brash ice in icebreaker-opened channel is considered in this study.

(1) Lindqvist empirical formula method:

$$R_{ice} = (R_c + R_B) \left(\frac{1 + 1.4V}{\sqrt{gh_{ice}}} \right) + R_s \left(\frac{1 + 9.4v}{\sqrt{gL}} \right) \tag{3}$$

where R_{ice} is the ice breaking resistance, V is the ship velocity, R_s is the submersion resistance, R_c is the crushing resistance, R_B is the bending resistance, h_{ice} is the ice thickness, v is the ice’s Poisson’s ratio, g is the gravitational acceleration. While Equation (3) is usually applied to level ice breaking, Lindqvist formula is modified as in [20] to calculate the ice resistance in brash ice (Crushing and bending strength of ice were assumed to be zero in broken brash ice) as shown in Equation (4).

$$\begin{aligned}
 R_{ice} &= R_s \cdot \left(1 + 9.4 \cdot \frac{v}{\sqrt{gL}} \right) \\
 &= (\rho_w - \rho_s) g h_{ice} B \cdot \left[T \cdot \frac{B+T}{B+2T} + \mu \right. \\
 &\quad \cdot \left(0.7L - \frac{T}{\tan(\varphi)} - \frac{B}{4 \tan(\alpha)} \right) \\
 &\quad \left. + T \cos(\varphi) \cos(\psi) \sqrt{\frac{1}{[(\sin\varphi)^2] + \frac{1}{(\tan\alpha)^2}} \right] \cdot \left(1 + 9.4 \cdot \frac{v}{\sqrt{gL}} \right)
 \end{aligned} \tag{4}$$

where R_{ice} is the ice resistance, R_s is the submersion resistance, h_{ice} is the ice thickness, v is the ice’s Poisson’s ratio, g is the gravitational acceleration. ρ_w is the density of sea water, ρ_s is the density of sea ice, T is the ship draught, L is the ship length between perpendiculars. B is the ship breadth, ψ is the normal angle, φ is the stem angle, α is the waterline entrance angle, μ is the coefficient of friction.

(2) FSICR rules formula:

$$R_{CH} = C_1 + C_2 + C_3 C_\mu (H_F + H_M)^2 (B + C_\psi H_F) + C_4 L_{PAR} H_F^2 + C_5 \left(\frac{LT}{B}\right)^3 \frac{A_{wf}}{L} \quad (5)$$

$$C_1 = f_1 \frac{BL_{PAR}}{2\frac{T}{B} + 1} + (1 + 0.021\varphi_1)(f_2 B + f_3 L_{BOW} + f_4 BL_{BOW}) \quad (6)$$

$$C_2 = (1 + 0.063\varphi_1)(g_1 + g_2 B) + g_3 \left(1 + 1.2\frac{T}{B}\right) \frac{B^2}{\sqrt{L}} \quad (7)$$

$$C_3 = 845 \text{kg}/(\text{m}^2 \text{s}^2) \quad (8)$$

$$C_4 = 42 \text{kg}/(\text{m}^2 \text{s}^2) \quad (9)$$

$$C_5 = 825 \text{kg}/\text{s}^2 \quad (10)$$

$$C_\mu = 0.15 \cos \varphi_2 + \sin \psi \sin \alpha \quad (11)$$

$$C_\psi = 0.047 \cdot \psi - 2.115 \quad (12)$$

$$\begin{aligned} H_M &= 1.0 \text{ for ice classes IA and IA Super} \\ &= 0.8 \text{ for ice class IB} \\ &= 0.6 \text{ for ice class IC} \end{aligned} \quad (13)$$

$$H_F = 0.26 + (H_M B)^{0.5} \quad (14)$$

where R_{CH} is ice resistance; $C_1, C_2, C_3, C_4, C_5, C_\mu, H_M, C_\psi, H_F$ are coefficients; B is ship beam (m); L_{PAR} is the length of the parallel midship body (m); T is actual ice class draughts of the ship (m); A_{wf} is the area of the waterline of the bow (m²); L is the length of the ship between the perpendiculars (m); $f_1 = 23 \text{ N/m}^2$; $f_2 = 45.8 \text{ N/m}^2$; $f_3 = 14.7 \text{ N/m}^2$; $f_4 = 29 \text{ N/m}^2$; $g_1 = 1530 \text{ N/m}^2$; $g_2 = 170 \text{ N/m}^2$; $g_3 = 400 \text{ N/m}^2$; L_{BOW} is the length of the bow (m); α is the angle of the waterline at $B/4$ (°); φ_1 is the rake of the stem at the centerline (°); and φ_2 is the rake of the bow at $B/4$ (°). The characteristic parameter values of specific length and angle are shown in Figure 1.

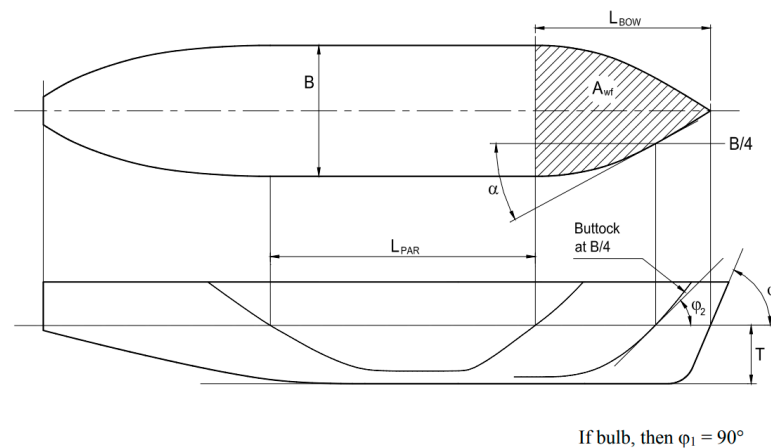


Figure 1. Characteristic parameter value.

In this study, when applying Lindqvist and FSICR formulas, the same calculation parameters are used. The specific parameters used to calculate ice resistance in this paper are shown in Table 2.

Table 2. Calculation parameters of different bow forms (Linqvist method and FSICR method).

Name	Traditional Icebreaker Bow Specific Value	Semi Bow Specific Value	EEDI Type of Bow Form Specific Value
φ_1	40.15	90.00	80
φ_2	33.38	32.41	48.26
α	28.98	30.92	46.23
v	0.3	0.3	0.3
ρ_s	900 kg/m ³	900 kg/m ³	900 kg/m ³

2.3. Main Engine Power Calculation Based on EEDI Stages

The EEDI [21] is calculated using Equation (15), and the effect of ice class is added to the calculation. The allowable EEDI value of each phase is calculated, and then the main engine power at different EEDI stages is calculated. The power obtained by the attained EEDI value is used as the criterion for the ship’s main engine power in ice area.

$$\frac{\left(\prod_{j=1}^n f_j\right) \left(\sum_{i=1}^{nME} P_{ME} \cdot C_{FME(i)} SFC_{ME(i)}\right) + (P_{AE} \cdot C_{FAE} SFC_{AE}) + \left(\left(\prod_{j=1}^n f_j \cdot \sum_{i=1}^{nP\pi} P_{P\pi(i)} - \sum_{i=1}^{nef} f_{ef(i)} P_{AEef(i)}\right) \cdot C_{FAE} SFC_{AE}\right) - \left(\sum_{i=1}^{nef} f_{ef(i)} P_{ef(i)} \cdot C_{FME} SFC_{ME}\right)}{f_i \cdot f_c \text{ Capacity} \cdot V_{ref} \cdot f_w} \tag{15}$$

For the explanation of the specific parameters of Equation (15), please refer to [22]; it is mainly composed of the following parts:

$$\frac{\text{Main Engine(s)+Auxiliary Engine(s)+Auxiliary Energy Saving Technology(s)} - \text{Main Engine Energy Saving Technology(s)}}{\text{Transport Work}} \tag{16}$$

In this article, we mainly consider the attained EEDI calculation under the main engine power:

$$\frac{\left(\prod_{j=1}^n f_j\right) \left(\sum_{i=1}^{nME} P_{ME} \cdot C_{FME(i)} SFC_{ME(i)}\right)}{f_i \cdot f_c \text{ Capacity} \cdot V_{ref} \cdot f_w} \tag{17}$$

where V_{ref} is ship speed, Capacity is ship’s load weight, SFC_{ME} is certified specific fuel consumption [g/kWh], C_{FME} is non-dimensional conversion factor between fuel consumption and CO₂ emission, f_j is correction factor to account for ship specific design elements, e.g., ice classed ships, shuttle tankers, f_i is capacity factor, f_c is cubic capacity correction factor for certain ship types, f_w is non-dimensional coefficient indicating the decrease of speed in representative sea conditions, P_{ME} is rated installed power (MCR) for each main engine [kW].

3. Calculation Model Description

The ship proto hull form used in this paper is “MV Xue Long”. The shape of the midbody and stern of the ship is kept unchanged, and three different ship hull forms are established by changing the bow forms.

The ship has a displacement of about 21,025 tons and a maximum speed of 17.9 knots in open water. However, in order to meet EEDI requirements, the actual speed must be less than 15 knots [21]. Therefore, this paper uses 15 knots as the calculation base when calculating the main engine power in open water (the power required in open water is estimated based on maximum continuous rating (MCR) of 85%).

The bow forms used in this article were mainly:

1. Traditional icebreaker bow (it had higher icebreaking performance when navigating in an ice area).
2. Semi bow (it had good resistance performance when sailing in the scattered ice area and open water area).

- EEDI type of bow form (its original intention was to reduce the resistance when sailing in open water).

Semi bow and EEDI type of bow form were designed on the basis of [23]. In the design, the actual bow form model, which is a traditional icebreaker ship, was used as the mother model [24], and semi-parametric modeling method was used for deformation to obtain the other two bow forms.

3.1. Traditional Icebreaker Bow

For traditional icebreaker bow form (Figure 2), the bow shape has good ice-going capabilities and is capable to break level ice. The stem angle is quite moderate being about 30 degrees. The main dimensions of this bow form are shown in Table 3.

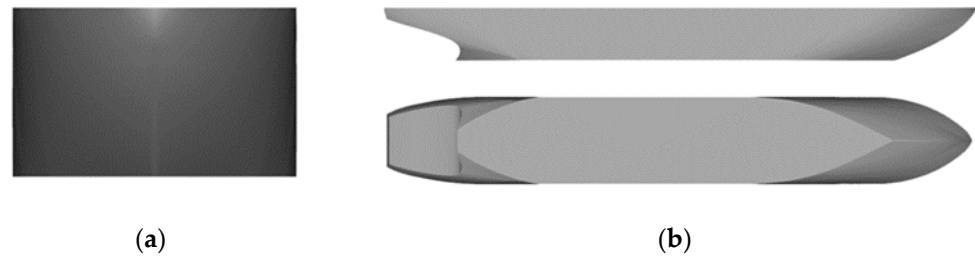


Figure 2. Ship model of traditional icebreaker bow. (a) Front view, (b) Top view and side view.

Table 3. Ship parameters of traditional icebreaker bow.

Name	Value
Length between perpendicular (L_{pp})	141.84 m
Width (B)	22.6 m
Depth (D)	13.5 m
Draft (T)	9.0 m

3.2. Semi Bow

The new bow shape (Figure 3) is designed to accommodate some open water characteristics with a little ice breaking capability. This is a typical bulbous bow. The main dimensions of this bow form are shown in Table 4. It is to be noted that the draft is to be set so that the bulb is submerged under waterline to avoid impact with ice, since bulb is not suitable for ice impact.

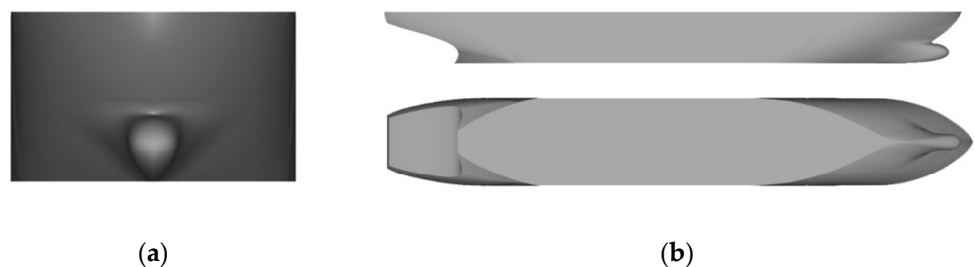


Figure 3. Ship model of semi bow. (a) Front view, (b) Top view and side view.

Table 4. Ship parameters of semi bow.

Name	Value
Length between perpendicular (L_{pp})	141.84 m
Width (B)	22.6 m
Depth (D)	13.5 m
Draft (T)	9.0 m

3.3. EEDI Type of Bow Form

The EEDI type of bow form (Figure 4) is mainly designed to deal with energy saving and emission reduction issues for open water. However, this hull form of bow is almost always a vertical bow. When encountering sea ice, it does not have the ability to sustain ice load damage, so it is a bow form with poor ice-going capability. The main dimensions of this form are shown in Table 5.

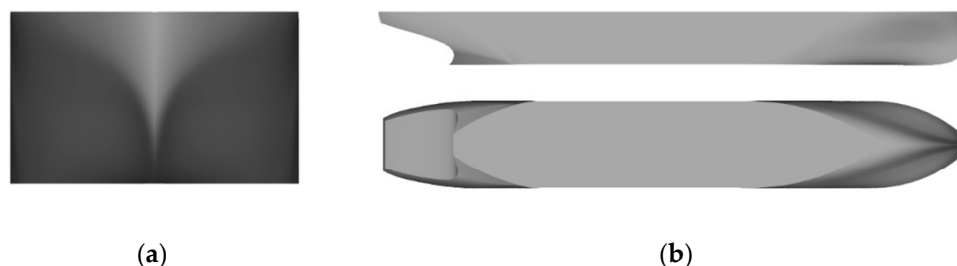


Figure 4. Ship model of EEDI type of bow form. (a) Front view, (b) Top view and side view.

Table 5. Ship parameters of EEDI type of bow form.

Name	Value
Length between perpendicular (L_{pp})	143.42 m
Width (B)	22.6 m
Depth (D)	13.5 m
Draft (T)	9.0 m

4. Calculation Results

4.1. CFD Calculation

4.1.1. CFD Numerical Verification

In this paper, DTMB5415 ship hull form was used for numerical verification, and all comparative experimental values were from the INSEAN [25] ship model experiment. The ship hull form of DTMB5415 is shown in Figure 5, and the ship hull form parameters are shown in Table 6.



Figure 5. DTMB5415 ship hull form.

Table 6. Main parameters of DTMB5415 ship model (scale ratio $\alpha = 22.832$).

Name	Value
Length between perpendicular (L_{pp})	5.72 m
Draft (T)	0.248 m
Width (B_{WL})	0.768 m
Wet area (S)	4.824 m ²
Displacement (Δ)	0.551 t
Barycentric coordinates	(2.89 m, 0 m, 0.2475 m)

First, the numerical uncertainty analysis is carried out, and three sets of grids are tested respectively. The numbers of grids are 5×10^5 , 7×10^5 and 9×10^5 . The incoming flow velocity during calculation is the design speed ($Fr = 0.28$).

The calculation results and comparison with INSEAN's experimental values are shown in Table 7 for different mesh sizes. By comparison, it can be found that the error between the resistance values calculated by the three sets of grids and the experimental values are within 5%. Then hull grid number of 7×10^5 is used to calculate the open water resistance

of the ship at three speeds ($Fr = 0.21, 0.28, 0.35$), and compared with INSEAN’s experimental value (Table 8). The error at all speeds was within 5%. This grid set 7×10^5 is used for later actual calculation, as this grid set can balance simulation accuracy and efficiency.

Table 7. Comparison of calculated resistance and experimental Value ($Fr = 0.28$).

Grid Quantity	R_T (N)	R_{T-EXP} (N)	Error/%
5×10^5	43.41	45.13	−3.81%
7×10^5	43.65	45.13	−3.28%
9×10^5	44.02	45.13	−2.46%

Table 8. Resistance value of the ship at each speed (number of grids was 7×10^5).

Fr	R_T (N)	R_{T-EXP} (N)	Error/%
0.20	21.29	21.56	−1.25%
0.28	43.65	45.13	−3.28%
0.35	76.23	80.61	−4.90%

4.1.2. CFD Calculation Result

In this paper, CFD calculations are performed on three hull forms of bows, their open water resistance values are obtained and the MCR value is calculated.

This paper use unstructured hexahedral mesh, grid encryption is performed at water plane: target cell sizes of height is 0.006 m, the max aspect ratio is 200. A boundary layer grid is set on the hull surface, first layer thickness is 0.00148 m, stretching ratio is 1.2, $y+$ [26] is 10, and the wall function is used. Finally, the watershed grid is obtained in Figure 6. In the calculation settings, the time step value is 0.014 s and the time step number is 1500.

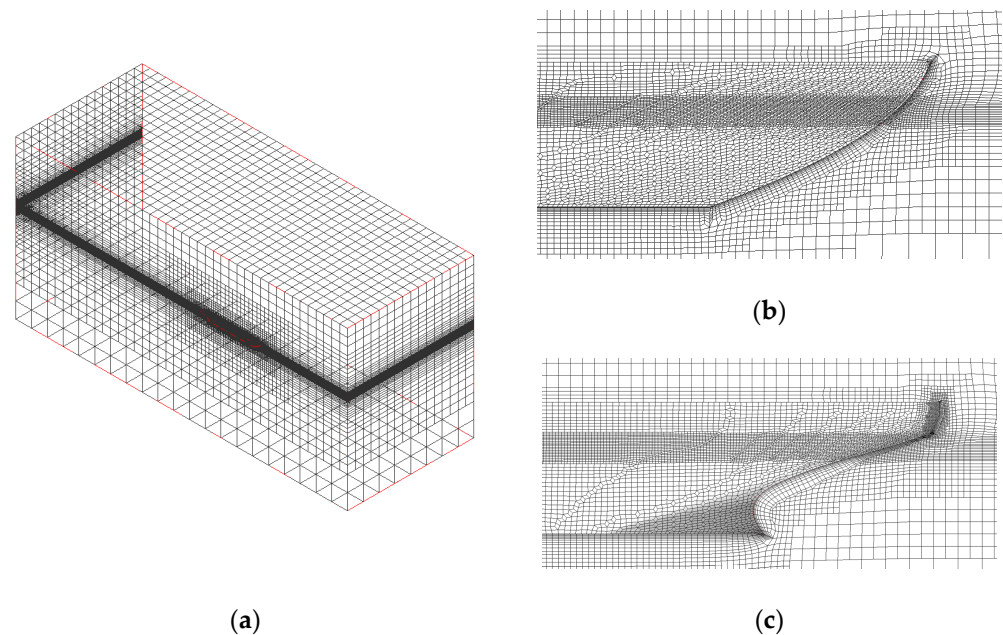


Figure 6. Ship hull mesh. (a) Grid of all areas, (b) Bow grid, (c) Stern grid.

The parameters and results for the traditional icebreaker bow are shown below as example. The ship hull form parameters are shown in Table 9. The calculated water surface wave height map under static water conditions is shown in Figure 7.

Table 9. Main parameters of traditional icebreaker ship model (scale ratio $\alpha = 40$).

Name	Value
Length between perpendicular (L_{pp})	3.546 m
Draft (T)	0.225 m
Width (B_{WL})	0.565 m
Wet area (S)	3.05 m ²
Displacement (Δ)	0.349 t
Barycentric coordinates	(1.7688 m, 0 m, 0.1889 m)

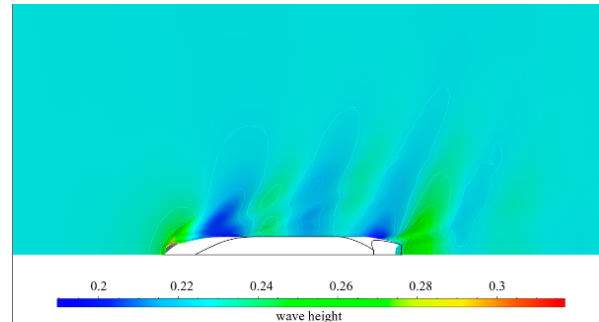


Figure 7. Water surface wave height.

The open water resistance value under 15kn of different bow forms are shown in Table 10. The results from ship model simulation are converted to the actual ship following the method of [27]. These values are used to calculate the ships’ MCR values in next section.

Table 10. Numerical resistance calculation.

Bow Form		Traditional Icebreaker Bow	EEDI Type of Bow Form	Semi Bow
Ship model (Velocity = 1.22 m/s)	R_{tm}	22.5 N	19.5 N	20.24 N
Real ship (Velocity = 7.716 m/s)	R_{ts}	1,215,214 N	1,018,334 N	1,065,580 N

4.2. Main Engine Power Calculation Results

The MCR, EEDI allowed power (Phase 2 and 3), required power calculated by Lindqvist method and FSICR of class 1C-1A Super ice class (Speed is set at 5 knots as required by FSICR) are calculated following the methods described above. Lindqvist and FSICR formula are used for the ice resistance calculation for main engine power and compared with the EEDI requirements in Figures 8–11 (a, b, c for different bow forms) for different ice classes. Figures 8–11 (d) are the comparisons for power requirements obtained from Lindqvist formula and EEDI requirements. In these figures, when the ratio is greater than 1, shown as green, EEDI requirement are satisfied for the considered ice classes and bow forms; when the ratio is less than 1, shown as red, then the EEDI requirement is not satisfied. In Figures 8–11 (d), “I2 (I3)” represents EEDI Phase 2 (Phase 3) for the traditional icebreaker bow, “S2 (S3)” represents EEDI Phase 2 (Phase 3) for the semi bow, “E2 (E3)” represent EEDI Phase 2 (Phase 3) for the EEDI bow form.

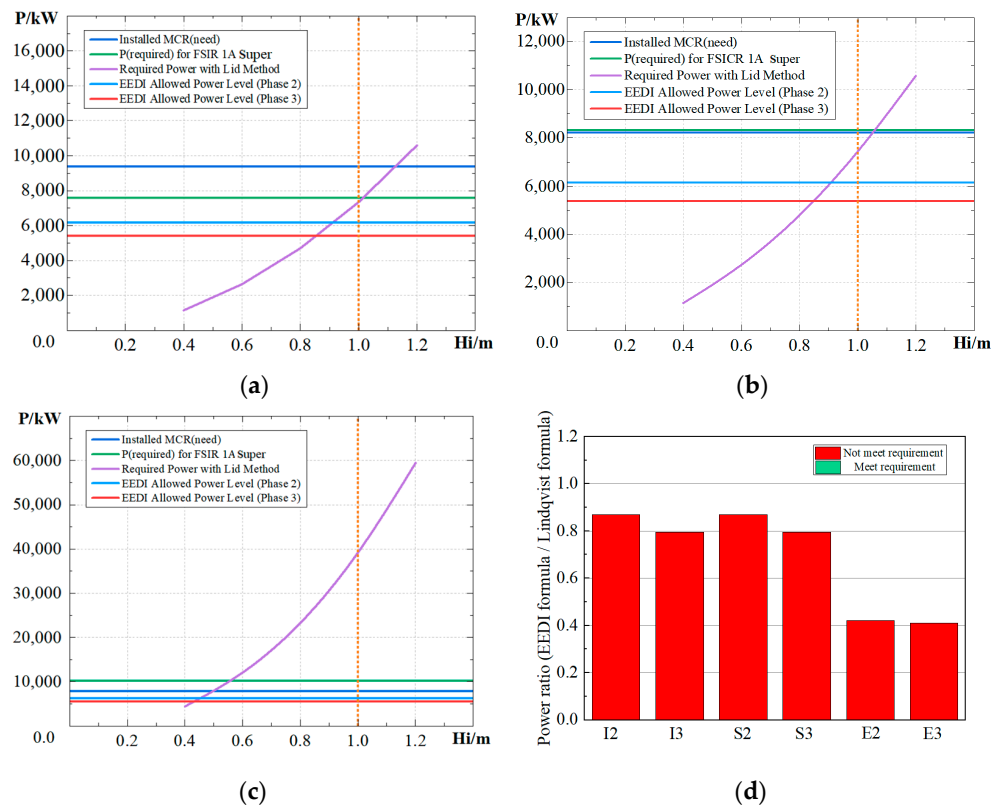


Figure 8. Power requirement results for 1A super. (a) Power of traditional icebreaker bow, (b) Power of semi bow, (c) Power of EEDI type of bow form, (d) Power requirement comparison.

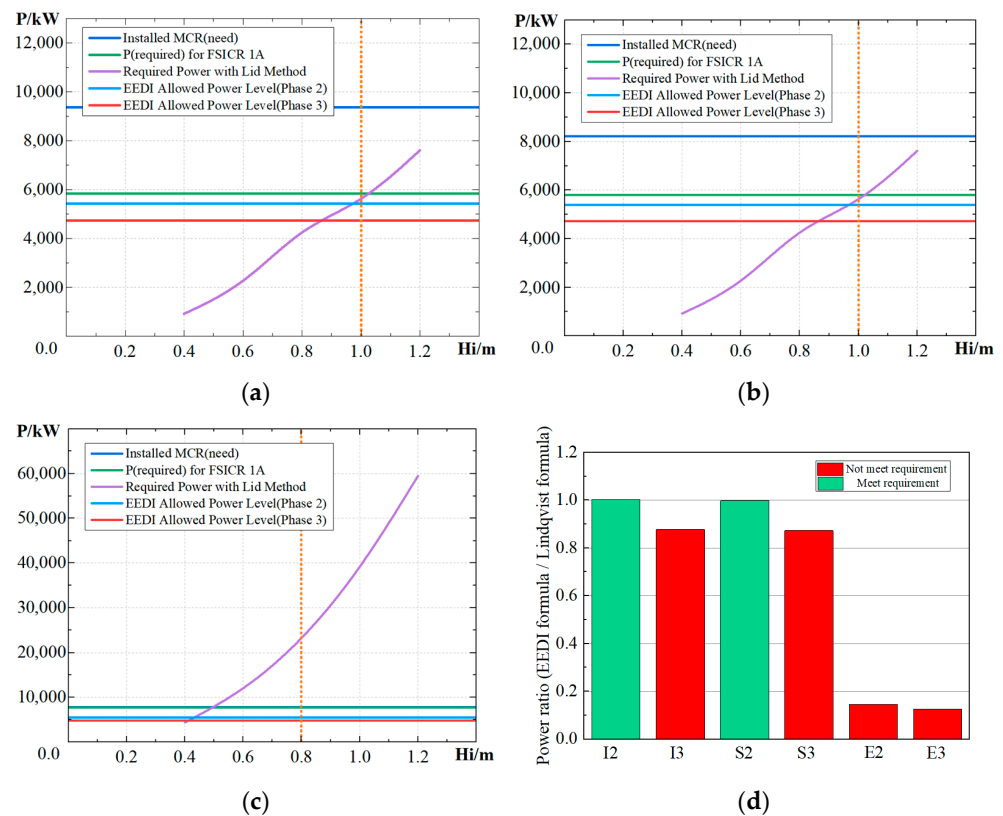


Figure 9. Power requirement results for 1A. (a) Power of traditional icebreaker bow, (b) Power of semi bow, (c) Power of EEDI type of bow form, (d) Power requirement comparison.

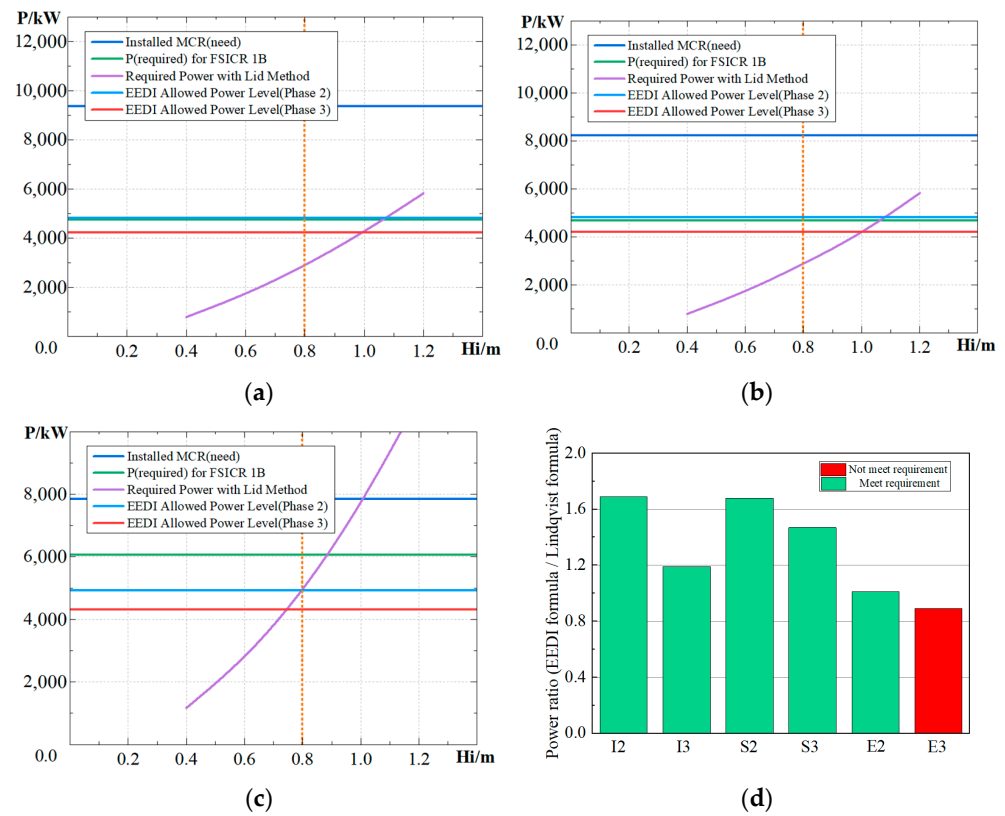


Figure 10. Power requirement results for 1B. (a) Power of traditional icebreaker bow, (b) Power of semi bow, (c) Power of EEDI type of bow form, (d) Power requirement comparison.

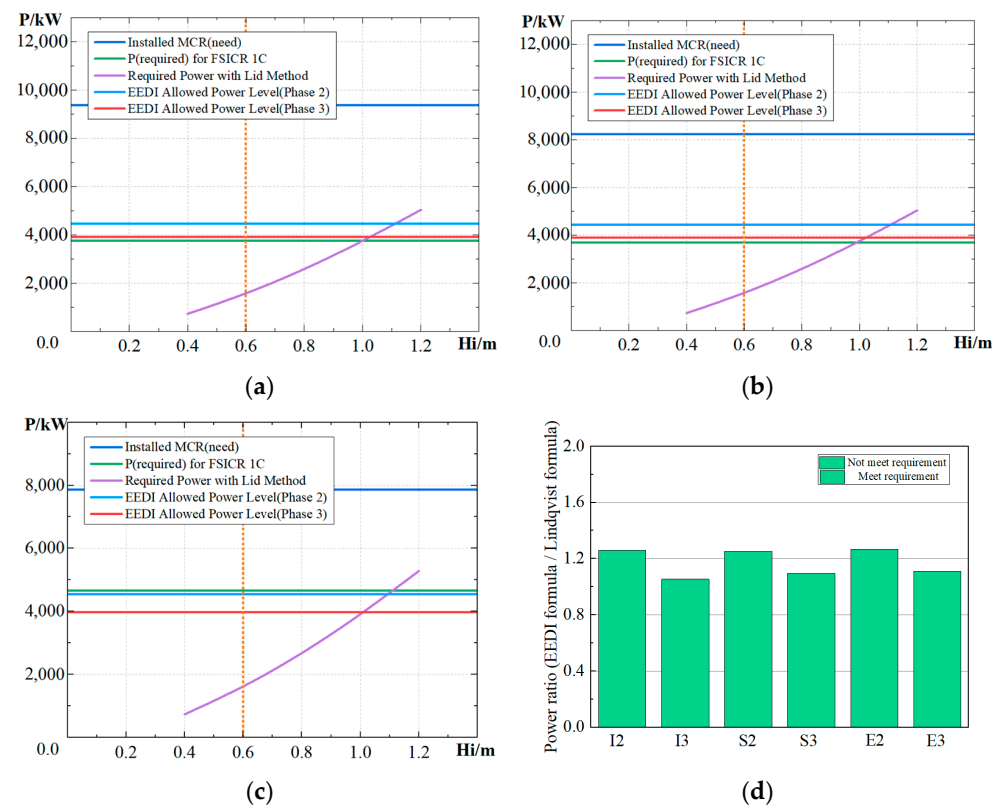


Figure 11. Power requirement results for 1C. (a) Power of traditional icebreaker bow, (b) Power of semi bow, (c) Power of EEDI type of bow form, (d) Power requirement comparison.

It is to be noted that for the semi bow, the bulb is assumed to be submerged under waterline to avoid direct contact with ice, thus the influence of the bulb to the ice resistance is not considered.

4.2.1. Ice Class 1A Super

Ice class 1A Super is assumed for 1 m thickness ice with 10 cm thickness consolidated layer as specified in FSICR. The maximum power allowed by EEDI Phase 2 is 6100–6300 kW, and the EEDI Phase 3 allowed power is 5400–5600 kW. As shown in Figure 8d, by comparing the power calculated by the Lindqvist method of different bow forms, it can be seen that none of the three bow forms meet the requirements under this ice class and the EEDI type of bow form has the worst ice navigation capability.

4.2.2. Ice Class 1A

FSICR defines the 1 m ice thickness for the 1A ice class. The maximum power allowed by EEDI Phase 2 is 5400–5600 kW. By comparing the power calculated by the Lindqvist method of different bow forms, it can be seen that the traditional icebreaker bow and semi bow just meet the power requirements for this phase.

The allowed power for EEDI Phase 3 is 5400–5600 kW. None of the three bow forms meet the EEDI Phase 3 requirements under this ice class and the EEDI type of bow form has the worst ice navigation capability.

4.2.3. Ice Class 1B

FSICR defines 0.8 m ice thickness for the 1B ice class. The maximum power allowed by EEDI Phase 2 is 4800–5000 kW. By comparing the power calculated by the Lindqvist method of different bow forms, it can be seen that all three bow forms meet the power requirements. The EEDI allowed power of Phase 3 is 4200–4400 kW. The traditional icebreaker bow and semi bow meet the requirements, but the EEDI type of bow form does not meet the requirements.

4.2.4. Ice Class 1C

FSICR defines the ice thickness of 0.6 m for 1C ice class. The max allowed power by EEDI Phase 2 is 4400–4600 kW, and the EEDI allowed power of the Phase 3 is 3900–4000 kW. By comparing the power calculated by the Lindqvist method of different bow forms, it can be seen that the all three bow forms meet the requirements under this ice class.

The results show that 1A Super ice classes for all considered bow shapes cannot meet the requirement by EEDI at Phase 2 and 3; For 1B and 1A ice class, some bow shapes can meet the EEDI requirement for all stages, but some cannot; For 1C class, all bow shapes can meet the EEDI requirements for all stages.

For the four ice classes, the power requirements when using the FSICR equation is on average higher than that of the Lindqvist method. Whether it meets the requirements of the EEDI Phases is demonstrated by red and green in Table 11 (The red area indicates that the power requirement is not met, and the green area indicates that the power requirement is met). It is to be noted that the power requirement calculated by FSICR formula is usually over-rated for large ships and alternative reduced power can be accepted with proper ice resistance calculation [19].

Table 11. Power comparison.

Phase2	EEDI Allowed Power				Required Power								Installed
	1A Super	1A	1B	1C	1A Super		1A		1B		1C		
					FSICR	Lid	FSICR	Lid	FSICR	Lid	FSICR	Lid	
Ice bow	6172.50	5425.33	4833.48	4460.77	7572.66	7344.07	5847.66	5414.04	4744.18	3563.17	3759.74	3703.58	9376.59
Semi bow	6145.26	5401.39	4812.15	4441.08	8330.58	7339.42	5802.20	5411.94	4687.89	2863.89	3695.41	3542.95	8222.02
EEDI bow	6289.29	5530.44	4928.77	4549.71	10,260.42	54,369.31	7690.13	38,285.35	6078.66	4868.00	4657.35	3591.88	7857.47
Phase3	EEDI Allowed Power				Required Power								Installed
	1A Super	1A	1B	1C	1A Super		1A		1B		1C		
					FSICR	Lid	FSICR	Lid	FSICR	Lid	FSICR	Lid	
Ice bow	5400.93	4747.16	4229.30	3903.17	7572.66	7344.07	5847.66	5414.04	4744.18	3563.17	3759.74	3703.58	9376.59
Semi bow	5377.10	4726.21	4210.63	3885.95	8330.58	7339.42	5802.20	5411.94	4687.89	2863.89	3695.41	3542.95	8222.02
EEDI bow	5503.12	4839.13	4312.67	3981.00	10,260.42	54,369.31	7690.13	38,285.35	6078.66	4868.00	4657.35	3591.88	7857.47

4.3. Main Engine Power under Different Pack Ice Concentration

In the above, the main engine power of ships sailing in ice regions is estimated under the EEDI rules for brash ice channel opened by escorting icebreaker. However, there may be also changes in pack ice concentration when ship traveling in ice covered water. Therefore, this paper needs to consider the main engine power variation values of three kinds of bow under different pack ice concentrations (9/10th and 7/10th). Because the EEDI type of bow form has poor ice-breaking ability, this section only calculates the Semi bow and traditional icebreaker bow. This article uses the DuBrovin [28] empirical formula.

In 1970, DuBrovin summarized and deduced the calculation formula for ice tank test data between 1950 and 1955. According to the empirical formula, the ice received in the ship model ice resistance calculation formula is:

$$R_{ice} = p_1 A + p_2 \Phi F_n \cdot n \tag{18}$$

where R_{ice} is the ice resistance of the ship; p_1 and p_2 are empirical coefficients, which depend on the distribution density of broken ice and the width of the broken ice channel; F_n is the Froude number; n is the power coefficient, which depends on the hull form of ship; A and Φ are defined as:

$$A = \frac{1}{4} B^2 \sqrt{r h_{ice} \rho_{ice}} \left(1 + 2 \frac{L}{B} f_0 \alpha_H \right) \tag{19}$$

$$\Phi = r h_{ic} \rho_{ice} B \left[f_0 + \tan \alpha_0 \left(\alpha_H + \frac{L}{B} \tan \alpha_0 \right) \right] \tag{20}$$

where ρ_{ice} is the density of sea ice; r is the density of broken ice, respectively; f_0 is the friction factor between the hull and the sea ice; α_0 is half of the incident angle of the water surface; and α_H is the rhomboid coefficient of the ship precursor. DuBrovin derived empirical coefficients p_1 and p_2 on the basis of the experimental data of different ice tanks ship model. All the parameters required by the empirical formula of the ship model in this paper are shown in Tables 12 and 13.

Firstly, the ice resistance under different ice thickness is calculated by DuBrovin formula, and then the power of ship’s main engine is calculated by Equation (1). As shown in Figure 12, the main engine power and power reduction rate of different ice concentration are obtained. By comparison, the main engine power required for 7/10 ice concentration is greatly reduced. Compared with the reduction of two bows, traditional icebreaker bow has greater advantages in energy saving.

Table 12. DuBrovin calculation parameters selected for this ship model (traditional icebreaker bow).

Parameter Hull Form	Value	Parameter Hull Form	Value
Ship width, B (m)	22.6	Length, L (m)	150.25
Distributed intensity of crushed ice, r	0.9/0.7	oefficient of friction, f_0	0.04
Ice thickness, h_{ice} /(m)	0.2–1.2	Half of the incident angle, $\alpha_0/(\circ)$	20.075
Crushed ice density, $\rho_{ice}/(\text{kg}/\text{m}^3)$	917	Precursor rhomboid coefficient, α_H	0.7176
Power factor, n	1.5		

Table 13. DuBrovin calculation parameters selected for this ship model (Semi bow).

Parameter Hull Form	Value	Parameter Hull Form	Value
Ship width, B (m)	22.6	Length, L (m)	150.25
Distributed intensity of crushed ice, r	0.9/0.7	Coefficient of friction, f_0	0.04
Ice thickness, h_{ice} /(m)	0.2–1.2	Half of the incident angle, $\alpha_0/(\circ)$	20.075
Crushed ice density, $\rho_{ice}/(\text{kg}/\text{m}^3)$	917	Precursor rhomboid coefficient, α_H	0.7039
Power factor, n	1.5		

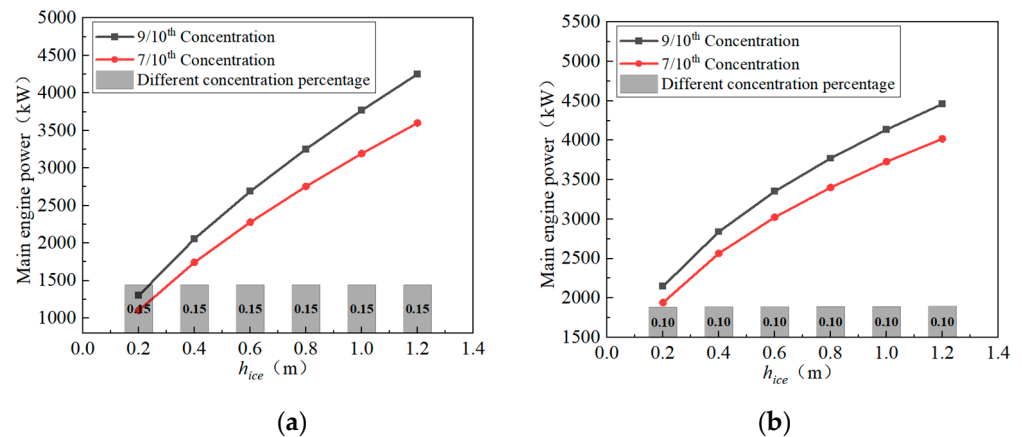


Figure 12. Power calculation with different pack ice concentration. (a) Traditional icebreaker bow, (b) Semi bow.

5. Conclusions

In this study, minimum required power for three different bow form derived from a typical icebreaker was calculated for 4 different Baltic ice classes, using the ice resistance from FSICR and Lindqvist formulas. The results are compared with EEDI maximum allowed power for Phase 2 and 3. The results show that the hull forms used in this paper cannot meet EEDI Phase 3 requirement for higher ice classes (1A and 1A super). Depending on the bow hull form, EEDI Phase 2 requirement may be met for these two ice classes. For lower ice classes (1B and 1C), EEDI Phase 2 and Phase 3 requirements are most likely to be achieved for these hull forms. Minimum power requirements for different pack ice concentration were calculated with different ice thicknesses and two bow forms. The results show that the reduced ice concentration makes EEDI requirements more easily satisfied for ice class ships.

In future research, first, the main engine power under the influence of auxiliary engine and main engine energy saving technology can be considered for EEDI requirement evaluation. Second, with parametric modeling of the bow, taking EEDI requirements as optimization target, an optimized bow form with energy saving suitable for ice navigation could be achieved.

Author Contributions: Conceptualization, Y.L. and S.L.; methodology, Y.L. and S.L.; software, Z.G., C.W. and C.L.; validation, Y.L. and S.L.; formal analysis, Z.G., W.S. and C.L.; investigation, Z.G., W.S. and C.L.; re-sources, S.L., Y.L.; data curation, Z.G.; Writing—original draft preparation, Y.L. and Z.G.; writing—review and editing, S.L.; visualization, Z.G.; supervision, S.L. and Y.L.; project administration, S.L. and Y.L. All authors have read and agreed to the published version of the manuscript.

Funding: This work was funded by the National Natural Science Foundation of China Youth Project (grant No. 51809029), the National Natural Science Foundation of China General Program Project (grant No. 52171293), the Ph.D. Scientific Research Fund of the Natural Science Foundation of Liaoning Province (grant No. 2019-BS-025), the High-Level Talent Innovation Support Program of Dalian (grant No. 2020RQ009), Key discipline project of Dalian Science and Technology Innovation Fund (grant No. 2020JJ25CY016), the Fundamental Research Funds for the Central Universities (grant No. 3132019306), and the Research Initial Foundation for Talents (grant No. 00253015).

Institutional Review Board Statement: Not applicable.

Informed Consent Statement: Not applicable.

Data Availability Statement: The data presented in this study are available on request from the corresponding author.

Conflicts of Interest: The authors declare no conflict of interest.

References

- Duan, C.; Wang, Z.; Dong, S. Study on the Multi-year Variations and Influencing Factors of Sea Ice in the Barents Sea. *Period. Ocean. Univ. China* **2019**, *148*, 148–162. (In Chinese) [[CrossRef](#)]
- Cai, M. In partial fulfillment of the requirements for the degree of Master of Engineering. Master's Thesis, Dalian Maritime University, Dalian, China, 2011. (In Chinese).
- Farkas, A.; Degiuli, N.; Martić, I.; Vujanović, M. Greenhouse gas emissions reduction potential by using antifouling coatings in a maritime transport industry. *J. Clean. Prod.* **2021**, *295*, 126428. [[CrossRef](#)]
- Balcombe, P.; Brierley, J.; Lewis, C.; Skatvedt, L.; Speirs, J.; Hawkes, A.; Staffell, I. How to decarbonise international shipping: Options for fuels, technologies and policies. *Energy Convers. Manag.* **2019**, *182*, 72–78. [[CrossRef](#)]
- Xing, H.; Spence, S.; Chen, H. A comprehensive review on countermeasures for CO₂ emissions from ships. *Renew. Sustain. Energy Rev.* **2020**, *134*, 110222. [[CrossRef](#)]
- Wang, H. Calculation and Analysis of Ship Energy Efficiency Design Index (EEDI). *Guangdong Shipbuild.* **2019**, *3*, 49–51. (In Chinese)
- Joung, T.-H.; Kang, S.-G.; Lee, J.-K.; Ahn, J. The IMO initial strategy for reducing Greenhouse Gas (GHG) emissions, and its follow-up actions towards 2050. *J. Int. Marit. Safety Environ. Aff. Shipp.* **2020**, *4*, 1–7. [[CrossRef](#)]
- Jeong, S.Y.; Jang, J.; Kang, K.J.; Kim, H.S. Implementation of ship performance test in brash ice channel. *Ocean Eng.* **2017**, *140*, 57–65. [[CrossRef](#)]
- Polakis, M.; Zachariadis, P.; de Kat, J.O. The energy efficiency design index (EEDI). In *Sustainable Shipping*; Springer: Berlin/Heidelberg, Germany, 2019; pp. 93–135.
- Westerberg, V.; Karlsson, R. *EEDI and Finnish-Swedish Ice Class Rules*; Winter Navigation Research Board, Research Report No. 88; Finnish Transport Safety Agency: Helsinki, Finland; Swedish Maritime Administration: Stockholm, Sweden, 2014.
- Lindeberg, M.; Kujala, P.; Sormunen, O.-V.; Karjalainen, M.; Toivola, J. Simulation model of the Finnish winter navigation system. In *Marine Design XIII*; CRC Press: Boca Raton, FL, USA, 2018; pp. 809–818.
- Marchenko, A.; Haase, A.; Jensen, A.; Lishman, B.; Rabault, J.; Evers, K.U.; Shortt, M.; Thiel, T. Laboratory investigations of the bending rheology of floating saline ice and physical mechanisms of wave damping in the HSVa Hamburg ship model basin ice tank. *Water* **2021**, *13*, 1080. [[CrossRef](#)]
- Wang, F.; Zhou, L.; Zou, Z.J.; Song, M.; Wang, Y.; Liu, Y. Study of continuous icebreaking process with cohesive element method. *Shipp. Technol. Pract. Shipp. Marit. Tech.* **2019**, *70*, 93–114. [[CrossRef](#)]
- Li, H.; Feng, Y.; Ong, M.C.; Zhao, X.; Zhou, L. An approach to determine optimal bow configuration of polar ships under combined ice and calm-water conditions. *J. Mar. Sci. Eng.* **2021**, *9*, 680. [[CrossRef](#)]
- Erceg, S.; Ehlers, S. Semi-empirical level ice resistance prediction methods. *Ship. Technol. Res.* **2017**, *64*, 1–14. [[CrossRef](#)]

16. Lindqvist, G.A. Straightforward method for calculation of ice resistance of ships. In Proceedings of the 10th Conference on POAC, POAC'89, Luleå University of Technology, Luleå, Sweden, 12–16 June 1989; pp. 722–735.
17. Riska, K. *Performance of Merchant Vessels in Ice in the BALTIC*; Helsinki University of Technology, Ship Laboratory: Helsinki, Finland, 1997.
18. Jeong, S.Y.; Choi, K.; Kang, K.J.; Ha, J.S. Prediction of ship resistance in level ice based on empirical approach. *Int. J. Nav. Archit. Ocean Eng.* **2017**, *9*, 613–623. [[CrossRef](#)]
19. ABS. *ABS Guidance Notes on Noise and Vibration Control for Inhabited Spaces*; American Bureau of Shipping: Spring, TX, USA, 2017.
20. Matala, R.; Skogström, T. *Brash Ice Channel Research*; Winter Navigation Research Board, Research Report No. 102; Aker Arctic Technology Inc.: Helsinki, Finland, 2017.
21. Kujala, P.; Kõrgesaar, M.; Kämäräinen, J. Evaluation of the limit ice thickness for the hull of various Finnish-Swedish ice class vessels navigating in the Russian Arctic. *Int. J. Nav. Archit. Ocean Eng.* **2018**, *10*, 376–384. [[CrossRef](#)]
22. Irclass. *Implementing Energy Efficiency Design Index*; Indian Register of Shipping: Mumbai, India, 2011; Volume 148, pp. 148–162.
23. Arctic, A. *Testing EEDI Bow Forms*; Aker Arctic Technology Inc.: Helsinki, Finland, 2018; Volume 9, pp. 11–12.
24. Lu, Y.; Gu, Z.H.; Liu, S.W.; Chuang, Z.J.; Li, Z.Y.; Li, C.Z. Research on optimization design of polar ship bows based on anti-ice performance. *Chuan Bo Li Xue/J. Ship Mech.* **2021**, *28*, 1040–1048. [[CrossRef](#)]
25. Olivieri, A.; Pistani, F.; Avanzini, A.; Stern, F.; Penna, R. *Towing Tank Experiments of Resistance, Sinkage and Trim, Boundary Layer, Wake, and Free Surface Flow around a Naval Combatant Insean 2340 Model*; IIHR Report No. 421; Iowa Institute of Hydraulic Research, The University of Iowa: Iowa, IA, USA, 2001; p. 56.
26. Ariff, M.; Salim, S.M.; Cheah, S.C. Wall Y + Approach for Dealing with Turbulent Flow Over a Surface Mounted Cube: Part 1—Low Reynolds Number. In Proceedings of the Seventh International Conference on CFD in the Minerals and Process Industries, CSIRO, Melbourne, Australia, 9–11 December 2009.
27. Grigson, C. Note on an accurate turbulent velocity profile for use at ship scale. *J. Ship Res.* **1989**, *33*, 162–168. [[CrossRef](#)]
28. DuBrovin, O.V.; Aleksandrov, M.; Moor, R. Calculation of broken ice resistance based on model testing. Ph.D. Thesis, University of Michigan, Ann Arbor, MI, USA, 1970.